Prediction of time variation of scour depth around spur dikes using neural networks

Hojat Karami, Abdollah Ardeshir, Mojtaba Saneie and S. Amin Salamatian

ABSTRACT

The maximum depth of scouring around spur dikes plays an important role in the hydraulic design process. There have been many studies on the maximum depth of scouring, but there is little information available on the time variation of scour depth. In this paper, the time variation of scouring around the first spur dike in a series was investigated experimentally. Experiments were carried out in four different bed materials under different flow intensities (U/U_{cr}). To achieve a time development of scouring around the first spur dike, more than 750 sets of experimental data were collected. The results showed that 70–90% of the equilibrium scour depths were occurring during the initial 20% of the overall time of scouring. Based on the data analysis, a regression model and artificial neural networks (ANNs) were developed. The models were compared with other empirical equations in the literature. However, the results showed that the developed regression model is quite accurate and more practical, but the ANN models by feed forward back propagation and radial basis function provide a better prediction of observation. Finally, by sensitivity analysis, the most and the least effective parameters, which affected time variation of scouring, were determined.

Key words | artificial neural networks, maximum scour depth, spur dike, time development of scouring

Hojat Karami (corresponding author)
Abdollah Ardeshir
S. Amin Salamatian
Department of Civil and Environmental Engineering,
Amirkabir University of Technology,
Tehran,
Iran
E-mail: *Hkarami1359@yahoo.com*

Mojtaba Saneie
Soil Conservation and Watershed Management Research Center,
Tehran,
Iran

NOTATION

a	Output of network
B	Width of the flume
b	Bias
D_{50}	Mean sediment grain size
D_{84}	84% finer particle diameter
D_{16}	16% finer particle diameter
d_{st}	Scour depth around first spur dike at time t
d_{se}	Equilibrium scour depth around the first spur dike
Fr	Froude number ($Fr = U/(gY)^{0.5}$)
F_d	Densimetric Froude number ($F_d = U/(\Delta g D_{50})^{0.5}$)
g	Gravitational acceleration
K_s	Relative roughness
L	Length of spur dike
L_R	Reference length ($L_R = L^{2/3}Y^{1/3}$)
n	Output of each neuron
N_s	Shape number
P	Input vector of neuron
p_i	ith input to neuron
Q	Volumetric discharge
S	Relative density of particles ($S = \rho_s/\rho$)
T	Time of equilibrium sour depth
T_S	Dimensionless time parameter ($T_s = tD_{50}$ $(\Delta g D_{50})^{0.5}/L^2$)
T_R	Dimensionless time of scour ($T_R = t\ (\Delta g D_{50})^{0.5}/L_R$)
t	Time of scouring
U	Average approaching flow velocity
U_{cr}	Critical velocity of approaching flow
u_*	Shear velocity of approaching flow
u_{*cr}	Critical shear velocity of approaching flow
W	Network parameter (weight) vector
w_i	ith weight of network
X	Spur spacing
Y	Approaching flow depth
ρ	Mass density of water

doi: 10.2166/hydro.2011.106

ρ_s Mass density of bed material
σ_g Standard deviation of bed material sediment ($\sigma_g = (D_{84}/D_{16})^{0.5}$)
$\varnothing$ Angle of repose of sediment particles
Δ relative density ($\Delta = S - 1$)

INTRODUCTION

Spur dikes are used to protect river banks from erosion and also to keep the main channel navigable. These structures are built from the river bank into the stream flow, usually in a group. A spur dike may be submerged during flood conditions or be exposed during the low flow. Spur dikes may be classified into two types: impermeable and permeable. Generally, the submerged condition is undesirable for impermeable spur dikes since the overtopping flow may cause severe erosion and damage (Zhang 2005). A major concern around spur dikes is local scouring which can cause failure of these structures. The type of local scour is classified according to the mode of sediment transport in the approaching flow such as clear water or live-bed condition. Many experimental studies have been carried out to determine the maximum scour depth around the spur dikes. Ahmad (1953) identified the main effective parameters on maximum scour depth. Garde *et al.* (1961) stated that the Froude number and sediment size are effective parameters on the maximum scour depth. Laursen (1962) developed an empirical equation to predict maximum scour depth. Zaghloul (1983) concluded that maximum scour depth is significantly affected by the opening ratio of the channel and Froude number. Karami *et al.* (2008) investigated the protection of a series of spur dikes by adding a protective spur dike located at the upstream end of the first spur dike.

Generally spur dikes are arranged in a group to improve efficiency and a single spur dike is not commonly used in actual cases. Gisonni *et al.* (2005) recommended that spur spacing (X) should be between two and four times the spur length (L) to maintain flow recirculation and spur integrity; a spur length to river width ratio (L/B) up to 0.25 will result in a contraction effect of the spur arrangement on to the river flow and the spur alignment is usually 90°, that is, perpendicular to the river axis, with possible angles being between 60° and 120°. Also, Zhang (2005) recommended that the ratio of spur spacing and spur length (X/L) should be less than three to prevent the channel bank from erosion of the returning currents. He also found that the scour is insignificant after the fourth spur dike. In a series of consecutively built spur dikes, the first upstream spur dike should be built to be sturdier, because the secondary flow has a more destructive force on this structure. Suzuki (1989) suggested estimating the maximum scour depth at the first spur dike with any empirical formula for a single spur dike. Other spur dikes have little effect on the scour depth of the first spur dike.

Time duration is an important parameter in the prediction of scour depth around the first spur dike. Some equations for the prediction of time variation of scour depth around abutments and spur dikes are shown in Table 1.

In recent years, intelligent methods such as artificial neural networks (ANNs), genetic algorithms (GAs) and neuro fuzzy systems have been used widely to address various complex problems in different fields of engineering (Savic *et al.* 2009; Hsu 2011). Giustolisi & Savic (2009) studied the prediction of groundwater level variation by rainfall. They improved the evolutionary polynomial regression (EPR) strategy by using a multi-objective GA. Their results showed that the multi-objective approach is a

Table 1 | Some equations reported by other researchers to predict time variation of scour

Reference	Equation
Ballio & Orsi (2001)	$\frac{d_{st}}{d_{se}} = 1 - \exp\left[-0.028\left(\frac{tU}{(bY)^{0.5}}\right)^{0.28}\right]$
Oliveto & Hager (2002)	$\frac{d_{st}}{L_R} = 0.068 N_S \sigma_g^{-0.5} F_d^{1.5} \mathrm{Log}(T_R)$
Coleman *et al.* (2003)	$\frac{d_{st}}{d_{se}} = \exp\left[-0.07\left(\frac{U_{cr}}{U}\right)\left\lvert Ln\left(\frac{t}{T}\right)\right\rvert^{1.5}\right]$
Yanmaz & Kose (2007)	$\frac{d_{st}}{L} = 0.25 F_d^{0.85}\left(\frac{L}{Y}\right)^{0.15}(\mathrm{Log}T_s)^{0.6}$

Where t, time of scouring; d_{st}, scour depth at time t; d_{se}, equilibrium scour depth; T, time to reach equilibrium scour depth; U, flow velocity; U_{cr}, critical velocity for incipient motion for bed sediment movement; F_d, densimetric Froude number ($F_d = U/(\Delta g D_{50})^{0.5}$); D_{50}, mean diameter of bed sediment; Y, approach flow depth; L, abutment length perpendicular to the flow direction; b, abutment width; g, gravitational acceleration; S, relative density of particles ($\Delta = S - 1$); σ_g, standard deviation of bed sediment material ($\sigma_g = (D_{84}/D_{16})^{0.5}$); $T_R = t\,(\Delta g D_{50})^{0.5}/L_R$; T_s, dimensionless time parameter ($T_s = tD_{50}\,(\Delta g D_{50})^{0.5}/L^2$); N_s, shape number equal to 1.25 and $L_R = L^{2/3}Y^{1/3}$.

more feasible instrument for data analysis and model selection. Recently, ANNs have been applied to solve problems in various fields of hydrology and water resources (Evora & Coulibaly 2009; Islam 2010; Shamseldi 2010) and scour prediction (Dehghani *et al.* 2006; Farhoudi *et al.* 2010; Kazeminezhad *et al.* 2010; Muzzammil & Ayyub 2010). Liriano & Day (2001) used ANNs to predict scour depth at culvert outlets. The results showed that the ANNs can successfully predict the depth of scour with a greater accuracy than existing empirical formulas over a wider range of conditions. Azmathullah *et al.* (2005) developed ANNs for estimating the scour downstream of a ski-jump bucket and found that the ANN predictions were more appropriate than those given by traditional regression equations. They found that the ANN model using non-dimensional parameters gave better results to predict scour depth downstream of the ski-jump. Bateni *et al.* (2007) used the ANNs to estimate the time variation of scour depth around the bridge piers and found that the dimensional data produce better results than non-dimensional ones.

Although time variation is an important parameter in scouring around spur dikes, there are very few studies available on the time variation of scour around spur dikes and abutments. In this study, it has been observed that the first spur dike in a series is the most important one that needs protection. Therefore, the time for reaching the maximum local scour depth around the first spur dike has been investigated in different experimental conditions. The main objective of this study is to develop an empirical equation based on dimensional analysis which is applicable for engineers. Moreover, ANN models are developed to determine the time variation of local scouring. Then, the empirical equation and ANN models are compared with other literature equations. Finally, a sensitivity analysis is carried out to determine the relative significance of each independent parameter.

ARTIFICIAL NEURAL NETWORKS

An ANN is a mathematical tool, which tries to represent low-level intelligence in natural organisms and a flexible structure, capable of making a non-linear mapping between

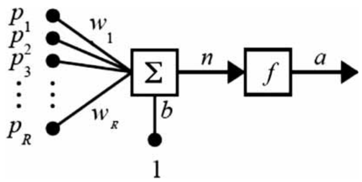

Figure 1 | Model of a neuron with multiple inputs.

input and output spaces. A neuron is the smallest unit of information processing; Figure 1 shows a neuron with R inputs. Considering $P = (p_1, p_2, \dots, p_R)$ as input vectors and $W = (w_1, w_2, \dots, w_R)$ as network parameters (weight) and the goal is to approximate a multi-variant function $f(x)$. The learning procedure is to find the best weight vector (W) to achieve the best approximation of $f(x)$.

n is the output of each neuron, as obtained from Equation (1).

$$n = \sum_{i=1}^{R} p_i w_i + b = W\underline{P} + b \tag{1}$$

where b is a bias which affects an n (output). From Figure 1 and Equation (1) the results are

$$a = f(W\underline{P} + b) \tag{2}$$

The function (f) is selective and it may be linear or non-linear. The common function for this purpose is the sigmoid function, which is given by

$$f_s(n) = sig(n) = \frac{1}{1 + e^{-cn}}, c > 0 \tag{3}$$

In this study a feed forward network (FFN) is used for estimating the time variation of scour depth around the first spur dike. In the FFN, nods are arranged in layers, the first layer is input data, the middle layers introduce hidden layers and the last layer is the output results. Determining the appropriate number of neurons in the hidden layers is an important aspect of an efficient network. Hecht-Nielsen (1988) suggested an upper limit of $(2i + 1)$ hidden layer neurons, where i is the number of input neurons. In this study, the number of neurons in the hidden layers was detected by using a trial and error method.

Input data should be normalized. There are various methods to normalize the data which have been adopted in the literature. Normalization is performed herein by using a linear scaling of raw data as follows

$$X_n = \frac{(X - X_{min})}{(X_{max} - X_{min})} \tag{4}$$

where X_n is the normalized value of X, and X_{max} is the maximum value and X_{min} is the minimum value of each variable of the original data. This normalization is not essential, but allows the network to be trained better.

EXPERIMENTAL SETUP AND PROCEDURES

All experiments were carried out in four flumes. The first three flumes (flume nos 1–3) had 0.6, 1.3 and 1.5 m width with 1 m depth and 30 m length respectively, and were located at the Soil Conservation and Watershed Management Research Center in Tehran. Flume no. 4 had 1 m width, 1 m depth and 14 m length and was located at the porous media laboratory of Amirkabir University of Technology. The test section, where the spur dikes were located in the flumes, was selected in a way that a uniform flow was established. To ensure, that a fully developed turbulent flow was reached in the upstream of the test sections, the velocity profiles were measured in all test cases. In flumes 1–3, four spur dikes and in flume 4, three spurs were installed. They were impermeable, non-submerged and perpendicular to the flow direction. The space between them was fixed and the spaces were equal to two times their length. A small reservoir was constructed at the downstream end of each flume to collect transported sediments. The flow discharge was regulated by an inlet valve. It was measured by a triangle weir at flume 1 and a rectangular weir at the flumes 2–4. Figure 2 shows views of the experimental flumes and spur dikes. Uniform bed sediments ($\sigma_g < 1.4$), consisting of sand (S) and gravel (G), with a thickness of 0.35 m were used. Table 2 shows details of the conducted experiments in which the parameters are defined as: B, width of the flume and Fr, Froude number, $Fr = U/(gY)^{0.5}$. To carry out each experiment, first the flume was gradually filled in order to entirely saturate the bed materials. Then, the sluice gate located at downstream of the flume, which controls the water level, was gradually lifted to adjust the desired discharge. Experiments were conducted with different values of U/U_{cr}. Clear-water condition ($U/U_{cr} < 1$) was satisfied in all experiments. Different values of U/U_{cr} were calculated with the following relationship presented by Lauchlan & Melville (2001)

$$\frac{U_{cr}}{u*_{cr}} = 5.75\,\mathrm{Log}\left(\frac{Y}{K_s}\right) + 6 \tag{5}$$

where u_{*cr} was obtained from the Shields diagram (Table 2) and K_s is equivalent roughness (equal to $2D_{50}$).

The time variation of scour depth around the first spur dike was carefully measured by an ultrasonic depth sounder with an accuracy of ±0.4 mm. The probe in this instrument had a diameter of 20 mm, emitting sound waves by a frequency of 2 MHz, with a sound wave resolution of ±0.37 mm in water at 20 °C. The time intervals for measurements were different, since the rate of scouring varied during the experiments. For instance, during the first hour of testing, scour depth was measured at intervals of 1 min while between the first and second hour, an interval of 5 min was selected. However, by considering the negligible scour rate, the last measurements were taken at an interval of more than 1 h. In this research, equilibrium depth of scour was defined based on Chiew (1992) as a depth with less than 1 mm change after 8 h of experimental run. Finally, 787 experimental data were collected from this study.

At the end of each experimental run, water was drained off from the flume with sufficient care to prevent any disturbance in the scour holes. Then the variations of bed profile around spur dikes were measured by a digital point gauge known as a laser bed profiler (LBP) with an accuracy of ±1 mm in width and ±0.1 mm in depth. Approximately more than 60,000 three-dimensional data related to bed variations around spur dikes in each experiment were measured by LBP.

EXPERIMENTS AND OBSERVATIONS

Figure 3 shows the variation of scour depth versus time for experiments S3, S4 and S5 (Table 2). This figure indicates

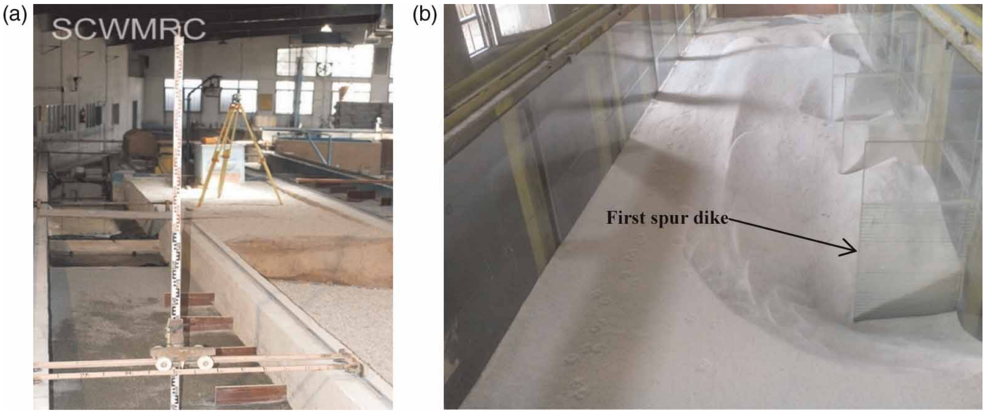

Figure 2 | A view of the experimental flume and installed spur dikes: (a) flume 2 and (b) flume 4.

Table 2 | Conditions of experiments

Test no.	B (m)	L (m)	D_{50} (mm)	σ_g	Y (m)	U (m/s)	u_{*cr} (m/s)	U/U_{cr}	Fr	F_d	T (min)	d_{se} (mm)
S1	0.6	0.18	0.19	1.28	0.1	0.167	0.0125	0.67	0.17	3.01	990	71
S2	0.6	0.18	0.19	1.28	0.08	0.208	0.0125	0.87	0.24	3.76	1,140	122
S3	1	0.25	0.91	1.38	0.15	0.23	0.0213	0.63	0.19	1.9	900	168
S4	1	0.25	0.91	1.38	0.15	0.31	0.0213	0.85	0.26	2.55	1,685	269
S5	1	0.25	0.91	1.38	0.15	0.35	0.0213	0.96	0.29	2.88	3,000	334
S6	1.3	0.39	1	1.39	0.035	0.22	0.0229	0.73	0.38	1.73	1,110	149
S7	1.3	0.39	1	1.39	0.045	0.256	0.0229	0.81	0.39	2.02	1,020	177
S8	1.3	0.39	1	1.39	0.055	0.28	0.0229	0.85	0.38	2.2	660	204
G1	1.5	0.45	3	1.37	0.076	0.263	0.0496	0.43	0.3	1.19	840	146
G2	1.5	0.45	3	1.37	0.098	0.306	0.0496	0.48	0.31	1.39	510	170
G3	1.5	0.45	3	1.37	0.117	0.342	0.0496	0.52	0.32	1.55	480	209

that scour depth reaches an equilibrium condition in a shorter time for lower flow intensities ($T = 900$ min, $U/U_{cr} = 0.65$) in comparison to higher values of flow intensity ($T = 1{,}686$ min, $U/U_{cr} = 0.85$). Measured at the same interval the maximum depth of scouring increases by increasing the U/U_{cr}. Figure 4 presents dimensionless scour depth (d_{st}/d_{se}) versus dimensionless time (t/T). From this figure, one can conclude that 70–90% of scouring occurred during the first 20% of the equilibrium time in all experiments in both sand and gravel bed materials. Therefore, the maximum rate of scouring occurred during the first hours of the experiments.

Figure 5 shows the profile of scour holes around the spur dikes which was measured by LBP in Test S3 (Table 2). In this test, the maximum scour depths around the first, second and third spur dike were 168, 16 and 45mm, respectively. The total volume of scour holes around spur dikes was about 0.0309 m^3, in which 95% of this value occurred around the first spur dike. Moreover, the following observations were made from the scour process during the tests.

1. In a series of consecutive parallel spur dikes, the maximum scour depths occurred around the first and the last spur dikes.
2. In the scour hole upstream of the spur dikes, a creeping motion of sediments occurred because of the downward flow. Downstream of the spur dikes, sediments were suspended and lifted owing to upward flow

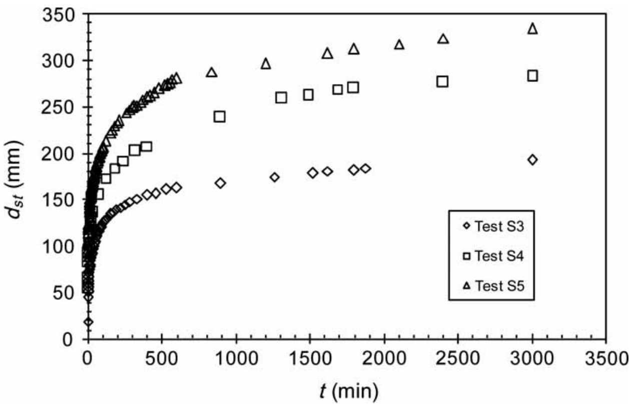

Figure 3 | Time variation of scour depth for Tests S3, S4 and S5.

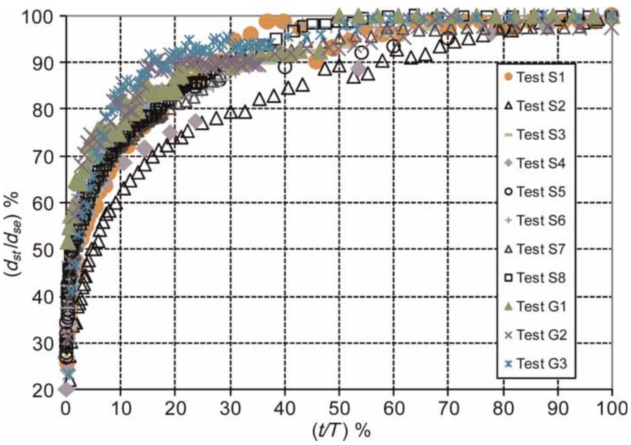

Figure 4 | Dimensionless scour depth (d_{st}/d_{se}) as function of the dimensionless time (t/T).

into the scour hole. Between two consecutive spur dikes, sediments were deposited because of the decrease in velocity.

3. In the test section, where spur dikes were located, the shear stress on the bed was more than critical shear stress causing the removal of sediments from the bed.
4. The location of the maximum scour depth always occurred near the upper corner of each spur dike and a conical shape of scouring in the nose of all spur dikes was formed.
5. The slope of the scour holes upstream was always more than the one downstream.
6. The average upstream slope of the scour hole was near the angle of repose of sediment particles (Ø), for example in tests S3, S4 and S5, $Ø = 30^\circ$ and the average upstream slope of the scour holes was near 30°. Similar results were observed at the slope of the scour hole around pier and abutment (Dey & Barbhuiya 2005).

ANALYSIS OF EXPERIMENTAL DATA (REGRESSION AND ANN MODELS)

A total of 787 test data were collected from the experiments. Out of that total, 590 data (75% of total data) have been randomly used for developing a regression model and ANN models. The remaining 197 data (25%) have been used for the validation of the regression model, ANN models and other empirical equations in literature.

The time variation of scour depth (d_{st}) can be written as a function of U, U_{cr}, t, T, D_{50} and d_{se}. A dimensional analysis was carried out and non-dimensional parameters of t/T, U/U_{cr} and F_d have been obtained for developing a regression model. Different non-linear regression models were developed. It was observed that F_d has no significant effect on the relative scour depth (d_{st}/d_{se}). Finally, it led to the following equation for estimation of time-dependent scour depth at the first spur dike

$$\frac{d_{st}}{d_{se}} = \left(\frac{t}{T}\right)^{0.16}\left(\frac{U}{U_{cr}}\right)^{-0.14} \tag{6}$$

Figure 6 shows good agreement between the measured and developed regression model in training and validation. The coefficient of determination for the training and validation of the model are $R^2 = 0.90$ and $R^2 = 0.86$ respectively. This figure indicates that 83% of the validation data are confined to ±10% limits. Therefore, Equation (6) is a practical and simple equation which can be used with high accuracy.

According to Figure 6, some discrepancy between the measured and predicted data can be observed at low values of d_{st}/d_{se}. Evidence showed that at the beginning of experiments, there were powerful vortices around the first spur dike; these vortices depend on many stochastic parameters which are difficult to determine. As these parameters were not entered in the regression model [Equation (6)], this apparent discrepancy between measured and predicted data for low d_{st}/d_{se} values was observed.

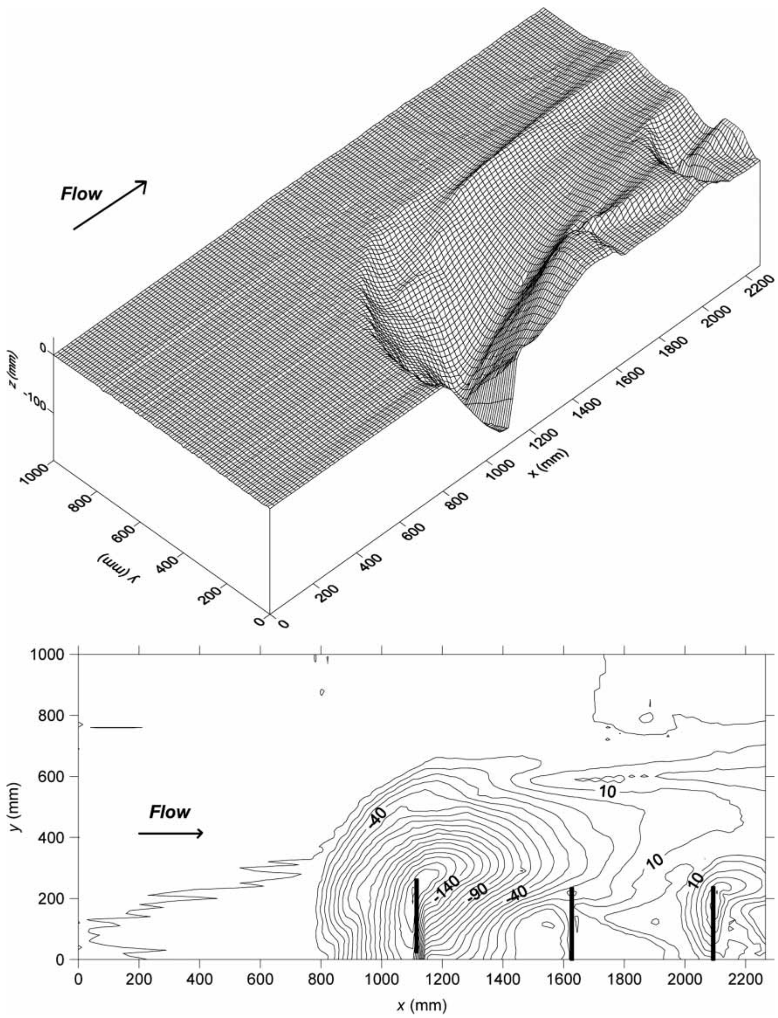

Figure 5 | Scouring profiles around spur dikes (Test S3).

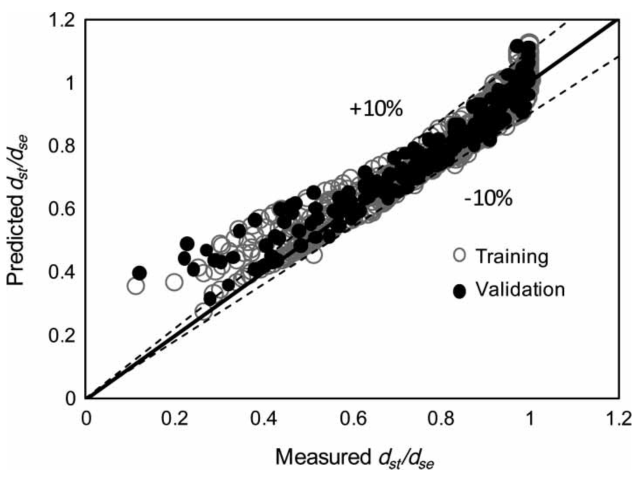

Figure 6 | Comparison between experimental data and regression model.

Three-quarters of all available data were randomly selected for training the networks and the remaining data were used to validate the networks as similarly for regression model. To evaluate the performance of the ANN models, they were divided in two groups (non-dimensional and dimensional model). This was done to investigate whether the use of the dimensional variables produced better results, than non-dimensional variables.

For both models, the feed forward back propagation (FFBP) and radial basis function (RBF) models were used to predict the time variation of scour depth. According to the Muzzammil & Siddiqui (2003) and Azmathullah et al. (2005) FFBP and RBF networks are suitable for hydraulic phenomena. The number of hidden layers, as well as the number of neurons is crucial for the successful application of ANN. The use of at least one hidden layer is generally recommended by the previous studies. By increasing the hidden layers the training process slows down without substantially improving the efficiency of the network. Kumar & Ray (1997) showed that the performance of a single hidden layer is better than double hidden layers for the rainfall-runoff modeling. Therefore, an ANN model with one input layer, one hidden layer and one output layer was selected. In the hidden layer, the sigmoid transfer function was used and in the output layer a linear transfer function was used. To compare the performance of the regression model, empirical equations and ANN models, the criteria of mean-absolute error (MAE), root-mean-square error (RMSE) and coefficient of determination (R^2) were used.

In the first group (non-dimensional data), the training of ANN was performed using U/U_{cr} and t/T as input data and the relative scour depth (d_{st}/d_{se}) as output data. To determine the number of neurons in the hidden layer, many networks were developed. The best networks with structural details are given in Table 3.

Table 4 shows performance parameters in different ANN models in training and validation stages. Results indicate that time variation of scour depth by ANN models in this study (FFBP and RBF models) have better performance than the regression model. However, the regression model is more practical than ANN models, but ANN models provide very accurate result when data are available [i.e. the performance of the regression model was improved 11% by FFBP model (Table 4)]. Non-dimensional models have been developed for the regression model case only since it is aimed at practical applications, where the data needed to train an ANN model are not available.

The training performance of the RBF and FFBP models are close to each other, but in the validation stage, results show that the FFBP model has better performance than the RBF model. Therefore, in this study the FFBP model is recommended to predict the time variation of scouring around spur dikes. Figure 7 shows good agreement between the measured and predicted values for the ANN model in both the training and validation stages. Most of the data are confined within ±10% along the trend line. To compare, Figures 6 and 7 showed that the FFBP model allows higher accuracy for low d_{st}/d_{se} values in comparison to the regression model. The ANN configuration for the FFBP model is shown in Figure 8.

In the second group (dimensional data), separate ANN models were developed using different input parameters (U, U_{cr}, D_{50}, t, T and d_{se}). It was observed that D_{50} and U_{cr} have similar effects on the time variation of scour depth (d_{st}), because U_{cr} and D_{50} are dependent [Equation (5)]. Therefore the training of the ANN was performed using U, D_{50}, t, T and d_{se} as inputs and the time variation of scour

Table 3 | Various algorithms of ANN scheme for non-dimensional parameters

	Network structure		
Neural network learning algorithm	**Number of input layer neurons**	**Number of middle layer neurons**	**Number of output layer neurons**
FFBP	2	8	1
RBF	2	29	1

Table 4 | Performance evaluations of various models for non-dimensional parameters

	Training stage			Validation stage		
Model	**MAE**	**RMSE**	**R^2**	**MAE**	**RMSE**	**R^2**
FFBP	0.026	0.033	0.97	0.026	0.034	0.97
RBF	0.027	0.036	0.96	0.028	0.044	0.95
Regression	0.041	0.054	0.9	0.048	0.067	0.86

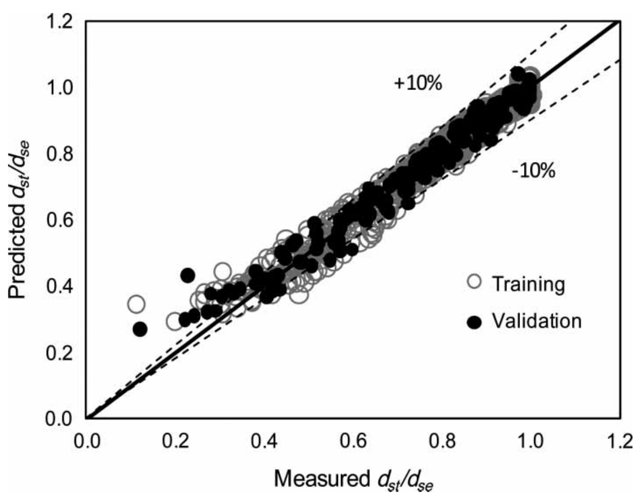

Figure 7 | Comparison of experimental data and FFBP model (using non-dimensional data).

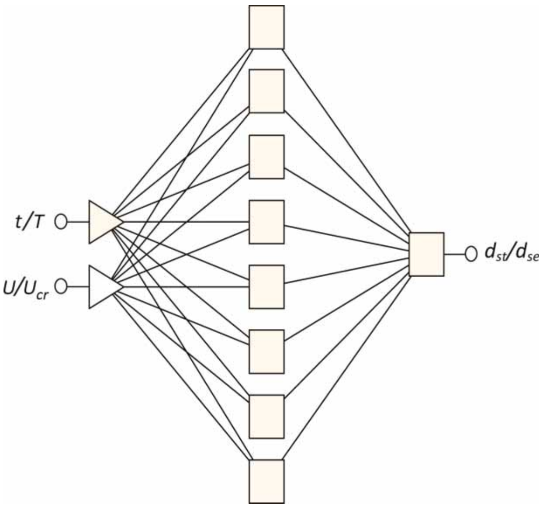

Figure 8 | Network architecture for FFBP model (using non-dimensional data).

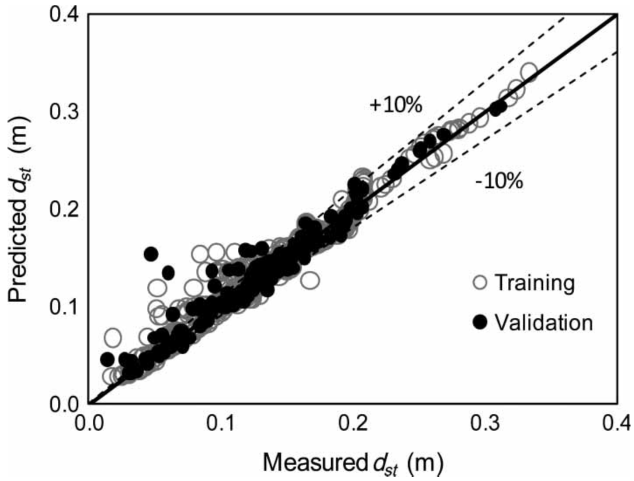

Figure 9 | Comparison of experimental data and the FFBP model (using dimensional parameters).

depth (d_{st}) as the output. Table 5 shows the best networks with structural details for the second group of ANN. In Table 6 performance parameters in different ANN models in training and validation stages are presented. According to Table 6, the FFBP model has a better performance than the RBF model. Therefore, the FFBP model is recommended to predict time variation of scouring in dimensional analysis. Figure 9 shows good agreement between measured and predicted values for the FFBP model in training and validation stages. The configuration of the network for the FFBP model is shown in Figure 10.

Table 5 | Various algorithms of the ANN scheme using dimensional parameters

	Network structure		
Neural network learning algorithm	Number of input layer neurons	Number of middle layer neurons	Number of output layer neurons
FFBP	5	9	1
RBF	5	31	1

Table 6 | Performance evaluations of various models for dimensional parameters

	Training stage			Validation stage		
Model	MAE	RMSE	R^2	MAE	RMSE	R^2
FFBP	0.0074	0.011	0.95	0.0082	0.014	0.93
RBF	0.0077	0.012	0.95	0.0096	0.015	0.92

COMPARISON OF REGRESSION MODELS WITH ANN MODELS

The ANN and regression models which are developed in this study and empirical equations were compared using validation data. First, the regression model in the present study was compared with other empirical equations. The results are shown in Table 7. According to Table 7, the Coleman *et al.* (2003) equation provides better prediction than other literature equations ($R^2 = 0.75$). The regression equation developed in this study, improved the results

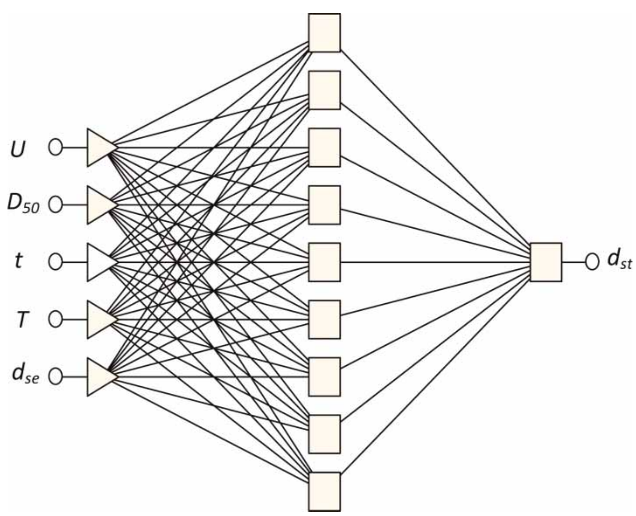

Figure 10 | Network architecture for the FFBP model (using dimensional data).

Table 7 | Comparison between various models to predict time variation of scour depth

Prediction model	MAE	RMSE	R^2
Ballio & Orsi (2001)	0.376	0.403	0.5
Oliveto & Hager (2002)	0.149	0.168	0.72
Coleman et al. (2003)	0.078	0.114	0.75
Yanmaz & Kose (2007)	0.114	0.144	0.51
Regression model (present study)	0.048	0.067	0.86
ANN (non-dimensional data)	0.026	0.034	0.97
ANN (dimensional data)	0.0082	0.014	0.93

($R^2 = 0.86$). The comparison of literature equations and Equation (6) is shown in Figure 11. Scattering of the measured time variation of scour depth data (Figure 11) indicates that the models that were developed for abutments may not provide suitable results for spur dikes. Moreover, the time variation of scouring around the first spur dike is more rapid than the time variation of scouring at the abutment. Equation (6) has better agreement by observed data than other empirical equations.

To evaluate the accuracy of the ANN models, a comparison between the regression and ANN models was undertaken. According to the literature and present results, it is concluded that the ANN models provide better prediction for time variation of scour than empirical equations. Comparison between Figures 6, 7 and 9 demonstrates that ANN models are more reliable than Equation (6) (Table 7). As can be concluded from Figures 7, 9 and Table 7, the non-dimensional parameter has better results than the dimensional parameter (Azmathullah et al. 2005). According to Figures 7 and 9, 94 and 86% of the validation data are confined to the ±10% limits for non-dimensional and dimensional parameters respectively.

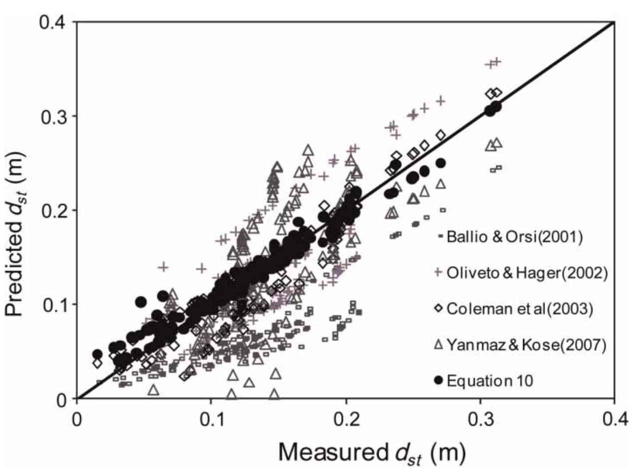

Figure 11 | Comparison of empirical equations for time variation of scour prediction.

SENSITIVITY ANALYSIS

Sensitivity analysis is commonly carried out to determine the relative significance of each independent parameter (input neurons) on the dependent parameter (output). The results of sensitivity analysis for non-dimensional and dimensional parameters are shown in Tables 8 and 9 respectively. Table 8 compares the ANN models with (U/U_{cr}) and (t/T) as independent parameters by an ANN model where one of the independent variables was removed from the model. Table 8 indicates that (t/T) and (U/U_{cr}) have the most and the least effect on the relative scour depth (d_{st}/d_{se}) respectively, as can be observed in Figure 4 also, whereas, the relative time (t/T) has more effects on the relative scour depth, as expected. Bateni et al. (2007) also observed similar results for time-dependent scour depth around bridge piers.

Table 8 | Sensitivity analysis results for non-dimensional parameters

	Training stage			Validation stage		
Model	MAE	RMSE	R^2	MAE	RMSE	R^2
ANN	0.026	0.033	0.97	0.026	0.034	0.97
ANN no U/U_{cr}	0.036	0.05	0.93	0.041	0.059	0.9

Table 9 | Sensitivity analysis results for dimensional parameters

	Training stage			Validation stage		
Model	MAE	RMSE	R^2	MAE	RMSE	R^2
ANN	0.0074	0.011	0.95	0.0082	0.014	0.93
ANN no U	0.0076	0.0127	0.93	0.0101	0.0159	0.89
ANN no D_{50}	0.0096	0.0131	0.91	0.0112	0.0168	0.87
ANN no t	0.0228	0.0317	0.32	0.0255	0.0353	0.17
ANN no T	0.0093	0.0138	0.92	0.0106	0.0161	0.88
ANN no d_{se}	0.0083	0.0123	0.94	0.0092	0.0152	0.91

Table 9 also indicates that the time of scouring (t) has the most effect on the ANN model and (d_{se}) has the least effect on the model, as can be observed in Figures 3 and 4 also. The effect of the dimensional variables on d_{st} are seen to be ranked (from highest to lowest) in the order t, D_{50}, T, U and d_{se}.

CONCLUSION

Time is one of the most important parameters in the prediction of scour depth around spur dikes; however, limited equations are available for the prediction of time variation of scour depth around spur dikes. In this research, the time variation of scour around the first spur dike in a series of spur dikes was experimentally tested under different values of (U/U_{cr}) and four sizes of sediment bed materials. The results indicated that the highest per cent of scouring ($d_{st}/d_{se} = 70$–90%) occurred during the initial times of scouring ($t/T = 20\%$). Between each two spur dikes, sediments were deposited because of a decrease in velocity. The location of maximum scour depth always occurred near the upper corner of the first spur dike. The average upstream slope of the scour hole was near the angle of repose of sediment particles (Ø).

From the collected experimental data, a new empirical equation was developed. The results indicated that presented empirical model has better prediction than other literature equations (with $R^2 = 0.86$). Also, the ANN models using non-dimensional data and dimensional data were developed. From this finding, the ANN models provide a much better prediction of time-dependent scour depth using non-dimensional data (with $R^2 = 0.97$) and ANN model using dimensional data provides time variation of scour depth with $R^2 = 0.93$. It has been demonstrated that non-dimensional parameters can provide better results in comparison with other literature equations and dimensional parameter.

REFERENCES

Ahmad, M. 1953 Experiments on design and behavior of spur-dikes. In *Proceedings of the International Hydraulics Convention*, University of Minnesota, Minneapolis, Minnesota, pp. 145–159.

Azmathullah, H. M., Deo, M. C. & Deolalikar, P. B. 2005 Neural networks for estimation of scour downstream of a ski-jump bucket. *ASCE J. Hydraul. Eng.* **131** (10), 898–908.

Ballio, F. & Orsi, E. 2001 Time evolution of scour around bridge abutments. *Water. Eng. Res.* **2** (4), 243–259.

Bateni, S. M., Jeng, D. S. & Melville, B. W. 2007 Bayesian neural networks for prediction of equilibrium and time-dependent scour depth around bridge piers. *Adv. Eng. Soft.* **38** (2), 102–111.

Chiew, Y. M. 1992 Scour protection at bridge piers. *J. Hydraul. Eng.* **118** (9), 1260–1269.

Coleman, S. E., Lauchlan, C. S. & Melville, B. W. 2003 Clear-water scour development at bridge abutments. *J. Hydraul. Res.* **41** (5), 521–531.

Dey, S. & Barbhuiya, A. K. 2005 Time variation of scour at abutments. *J. Hydraul. Eng. ASCE* **131** (1), 11–23.

Dehghani, A. A., Salamatian, S. A. & Ghodsian, M. 2006 Intelligent estimation of the maximum depth of scour hole around bridge piers in cohesive sediment using ANN. In *3rd International Conference on Scour and Erosion*, 14–17 October, The Netherlands.

Evora, N. D. & Coulibaly, P. 2009 Recent advances in data-driven modeling of remote sensing applications in hydrology. *J. Hydroinform.* **11** (3–4), 194–201.

Farhoudi, J., Hosseini, S. M. & Sedghi-Asl, M. 2010 Application of neuro-fuzzy model to estimate the characteristics of local scour downstream of stilling basins. *J. Hydroinform.* **12** (2), 201–211.

Garde, R. J., Subramanya, K. & Nambudripad, K. D. 1961 Study of scour around spur-dikes. *J. Hydraul. Div. ASCE* **87** (HY6), 23–37.

Gisonni, C., Hager, W. H. & Unger, J. 2005 Spurs in river engineering – a preliminary review. In *Proceedings of the 31st IAHR Congress, September 2005,* Seoul, Korea, pp. 1894–1901.

Giustolisi, O. & Savic, D. A. 2009 Advances in data-driven analyses and modelling using EPR-MOGA. *J. Hydroinform.* **11** (3–4), 225–236.

Hecht-Nielsen, R. 1988 Neurocomputing: picking the human brain. *IEEE Spectrum* **25** (3), 36–41.

Hsu, K. L. 2011 Hydrologic forecasting using artificial neural networks: a Bayesian sequential Monte Carlo approach. *J. Hydroinform.* **13** (1), 25–35.

Islam, A. S. 2010 Improving flood forecasting in Bangladesh using an artificial neural network. *J. Hydroinform.* **12** (3), 351–364.

Karami, H., Ardeshir, A., Saneie, M., Behzadian, K. & Jalilsani, F. 2008 Reduction of local scouring with protective spur dike. In *Proceedings of the World Environmental and Water Resources Congress ASCE*, 12–16 May, Hawaii USA.

Kazeminezhad, M. H., Etemad-Shahidi, A. & Yeganeh Bakhtiary, A. 2010 An alternative approach for investigation of the wave-induced scour around pipelines. *J. Hydroinform.* **12** (1), 51–65.

Kumar, D. N. & Ray, A. 1997 Application of artificial neural network for rainfall-runoff modeling. In *Proceedings of 24th National Conference on Fluid Mechanics and Fluid Power*, Calcutta, India, Vol. 1, 26–28 December, pp. D58–D61.

Lauchlan, C. S. & Melville, B. W. 2001 Riprap protection at bridge piers. *J. Hydraul. Eng.* **127** (5), 412–418.

Laursen, E. M. 1962 Discussion of study of scour around spur dikes. *J. Hydraul. Div. ASCE* **89** (HY3), 225–228.

Liriano, S. L. & Day, R. A. 2001 Prediction of scour depth at culvert outlets using neural networks. *J. Hydroinform.* **3** (4), 231–238.

Muzzammil, M. & Ayyub, M. 2010 ANFIS-based approach for scour depth prediction at piers in non-uniform sediments. *J. Hydroinform.* **12** (3), 303–317.

Muzzammil, M., Siddiqui, R. 2003 An artificial neural network model for scour prediction. In: *Advances in Civil Engineering, Prospective of Developing Countries. Vol. II*. (Parmar & Kumar, eds.). Allied Publishers Pvt. Limited, pp. 430–441.

Oliveto, G. & Hager, W. H. 2002 Temporal evolution of clear-water pier and abutment scour. *J. Hydraul. Eng.* **128** (9), 811–820.

Savic, D. A., Giustolisi, O. & Laucelli, D. 2009 Asset deterioration analysis using multi-utility data and multi-objective data mining. *J. Hydroinform.* **11** (3–4), 211–224.

Shamseldi, A. Y. 2010 Artificial neural network model for river flow forecasting in a developing country. *J. Hydroinform.* **12** (1), 22–35.

Suzuki, K. 1989 Hydraulic functions and problems of river training structures. *JSCE Summer Course in Hydraulic Engineering* A-4–4–A-4–22.

Yanmaz, A. M. & Kose, O. 2007 Time-wise variation of scouring at bridge abutments. *Sadhana* **32** (3), 199–213.

Zaghloul, N. A. 1983 Local scour around spur-dikes. *J. Hydrol.* **60** (1–4), 123–140.

Zhang, H. 2005 *Study on Flow and Bed Deformation in Channels with Spur Dyke*. PhD Thesis, Kyoto University, Japan.

First received 31 August 2010; accepted in revised form 4 January 2011. Available online 23 April 2011